International Journal of Chemical, Materials and Biomolecular Sciences
ISSN: 2415-6620
Vol:5, No:5, 2011

The Influence of Surface Potential on the Kinetics of Bovine Serum Albumin Adsorption on a Biomedical Grade 316LVM Stainless Steel Surface

Khawtar Hasan Ahmed and Sasha Omanovic*

***Abstract*—**Polarization modulation infrared reflection absorption spectroscopy (PM-IRRAS) in combination with electrochemistry, was employed to study the influence of surface charge (potential) on the kinetics of bovine serum albumin (BSA) adsorption on a biomedical-grade 316LVM stainless steel surface is discussed. The BSA adsorption kinetics was found to greatly depend on the surface potential. With an increase in surface potential towards more negative values, both the BSA initial adsorption rate and the equilibrium (saturated) surface concentration also increased. Both effects were explained on the basis of replacement of well-ordered water molecules at the 316LVM / solution interface, *i.e.* by the increase in entropy of the system.

***Keywords*—**adsorption, biomedical grade stainless steel, bovine serum albumin (BSA), electrode surface potential / charge, kinetics, PM-IRRAS, protein/surface interactions

I. Introduction

SPONTANEOUS adsorption of proteins onto solid-liquid interfaces is of great importance in many applications, such as in the food and pharmaceutical industry, biomaterials, biomedical implants, biosensors, drug delivery systems, *etc*. For instance, instantaneous adsorption of proteins from biological fluids to solid surfaces is extremely important in the field of biomaterials and implantable biomedical devices development, since it directly determines their biocompatibility (cell/surface interactions, positive and negative immune responses, blood coagulation, bacterial adhesion, *etc*.)[1, 2]. Protein adsorption has been, for example, also investigated in the field of development of medical electrical devices, such as biosensors and electrodes. It has been noted that protein adsorption on these (electrode) surfaces has a negative influence on the detection of electrical signal, thus influencing analysis of clinical samples[3]. However, in some cases adsorption of specific proteins and enzymes on surfaces is beneficial, such as in the immobilization of detection enzymes or antibodies/antigens on biosensor or immunosensor surfaces, respectively[4].

* (corresponding author): S.Omanovic is with the Department of Chemical Engineering, McGill University, 3610 University Street, Montreal, QC, H3A 2B2, Canada (sasha.omanovic@mcgill.ca)

K.H.Ahmed was with the Department of Chemical Engineering, McGill University, 3610 University Street, Montreal, QC, H3A 2B2, Canada (khawtar.ahmed@mail.mcgill.ca)

Researchers have applied a range of experimental techniques to study various aspects of protein interaction with solid surfaces, including the solution-depletion method[5-7], enzyme-linked immunosorbent assay (ELISA)[8, 9], radiolabelling[3, 10, 11], various optical techniques such as ellipsometry[12-14], total internal reflection fluorescence (TIRF)[15], optical waveguide lightmode spectroscopy (OWLS)[13, 16], surface plasmon resonance (SPR)[17, 18] and neutron reflectivity (NR)[19, 20]. Electrochemical quartz crystal nanobalance (EQCN)[21, 22] and quartz crystal microbalance (QCM)[13, 23] have also been used. Ultra-high-vacuum techniques, such as X-ray photoelectron spectroscopy (XPS)[24, 25], time-of-flight static secondary ion mass spectroscopy (TOF-SIMS)[26], surface matrix assisted laser desorption ionization time-of-flight mass spectroscopy (surface-MALDI-TOF-SIMS) [27] and scanning tunnelling microscopy (STM)[28] have been used. In addition, imaging techniques, such as atomic force microscopy (AFM) and scanning electron microscopy (SEM), have been employed to observe the conformation of surface adsorbed proteins, as well as their adsorption patterns[1, 15, 29-31]. Infrared spectroscopy (IR) methods have been used to not only obtain quantitative information of the amount of protein adsorbed, but also to gain insight on the adsorbed proteins' conformation. These include attenuated total reflection Fourier transform IR (ATR-FTIR)[2, 10, 32], grazing angle FTIR (GA-FTIR)[10, 33] and the relatively new technique of polarization modulation infrared reflection absorption spectroscopy (PM-IRRAS)[34, 35], that has also been used in the research presented here. Omanovic and Roscoe have applied electrochemical techniques, such as electrochemical impedance spectroscopy (EIS) and cyclic voltammetry (CV), to study the adsorption of a range of proteins on electrode surfaces[21, 36-41].

From the above presented, it is quite obvious that studying interaction of proteins with solid surfaces is of extreme importance in many fields. In particular, one should first understand fundamental phenomena that govern this process, such as the influence of physico-chemical properties of the surface (surface wettability and charge, van der Waals, electrostatic and hydrogen bonding forces, *etc*.) on the protein adsorption. For example, the influence of surface-charge has been investigated by modifying various surfaces (metallic, polymer, ceramic) with self-assembled monolayers (SAM's,

usually functionalized alkanethiols). However, it should be noted that by applying this approach, it is not possible to modulate only the surface charge while keeping other physico-chemical properties constant. For example, by switching between the negatively-charged COOH-modified SAM surface to the positively-charge NH_2-modified SAM surface, one also changes the surface chemistry, surface charge distribution, surface wettability and influences van der Waals and electrostatic forces (the surface conformation of SAM's is governed also by intermolecular interactions due to van der Waals forces). Thus, the subsequent protein adsorption is influenced not only by the surface charge and its distribution, but also by a range of other parameters.

This work aims at contributing to the field of research on protein/surface interactions by presenting and discussing results on the influence of surface charge of a biomedical grade 316LVM stainless steel on adsorption of a model protein, bovine serum albumin (BSA). In order to avoid the influence of surface chemistry and other physico-chemical parameters change (as in the case of SAM's use, as described above) on the BSA adsorption, the surface charge of 316LVM was modulated *in-situ* by electrochemical potentiostatic polarization of the surface in a BSA-containing electrolyte. The BSA adsorption kinetics was studied as a function of surface charge (i.e. surface potential). Characterization of BSA on the 316LVM surface was performed using PM-IRRAS. 316LVM was chosen as a substrate since this material is the most commonly used material for coronary stent fabrication and a range of other implants (fixation screws, hip prostheses, *etc*.), and is also frequently used in industry as a material for construction of various process equipment (reactors, storage tanks, heat-exchangers, filtration membranes, *etc*.). BSA was chosen since it is the most abundant protein in blood plasma, it has been extensively studied in the literature, and it has been frequently used as a model globular protein for studying protein/surface interactions relevant in a range of biomedical and industrial applications, thus enabling literature comparison[42].

II. Materials And Methods

All adsorption/desorption experiments were investigated in a 0.1 M of phosphate buffer (PB) solution of pH 7.4 and at temperature of 295 ±2 K. For adsorption kinetic experiments, a 1 g L^{-1} solution of bovine serum albumin (BSA, 99%; Sigma- Aldrich Co., Cat. No. A-0281) in 0.1 M PB was used. The response corresponding to time zero was measured in a BSA-free 0.1 M PB solution.

A 50 mL electrochemical glass cell was used in electrochemical experiments. The counter electrode (CE) was a 316L stainless steel wire. The reference electrode (RE) was a commercially available mercury/mercurous sulphate electrode. Three working electrodes were used in this cell; the first working electrode (WE_1) was a 316L stainless steel wire, while the remaining *two* working electrodes (WE_2) were two biomedical-grade 316LVM stainless steel samples (BSA adsorption samples), with dimensions of 2.4 cm × 1.2 cm × 0.1 cm, each hooked to a 316L wire to provide electrical contact. The purpose of WE_1 was to keep WE_2 under polarization while withdrawing the two WE_2 samples from the electrolyte for further analys. Namely, WE_2 was pulled out of the electrolyte while still being polarized at the required potential, which was necessary in order to prevent the samples potential drifting to open-circuit-potential during the removal from the electrolyte.

Prior to each experiment, all faces of both stainless steel adsorption samples (WE_2) were wet polished with SiC polishing paper, grit #4000. This was followed by abundant rinsing of the samples with deionized water, ultrasonication for five minutes in deionized water, three minutes in ethanol, and five minutes again in deionized water.

316LVM is material that passivates spontaneously, *i.e.* it forms a thin oxide film on its surface when in contact with moist atmosphere or any aqueous solution. The physico-chemical properties of this passive film depend on the sample exposure time to the air, electrolyte, and on the electrochemical passivation potential. Thus, in order to ensure that 316LVM samples were uniform, reproducible and of the same surface topography and physico-chemical properties, the samples were electrochemically treated by cyclic polarization in 0.1M PB after polishing, i.e. prior to each protein adsorption experiment. Fifty cyclic sweeps were made between -1.5 and +0.9 V, at a scan rate of 500 mVs^{-1}.

PM-IRRAS was used in this research to investigate interaction of BSA (adsorption kinetics) with a 316LVM stainless steel surface, as a function of the surface charge (potential). More detail on the use of PM-IRRAS for investigation of protein/surface interactions, could be found in our previously published work[43].

Kinetics of adsorption of BSA was performed in an electrochemical cell containing a phosphate solution of BSA, pH 7.4. Desired constant potential was first applied to the electrochemical cell containing WE_1, CE and RE, followed by immersion of the two electrochemically-treated 316LVM samples (WE_2) for a pre-determined length of time before being removed and rinsed with abundant deionized water for the subsequent PM-IRRAS analysis. For the initial point (time zero), this procedure was performed in a BSA-free 0.1 M PB solution (control).

Following protein adsorption and rinsing, the samples were dried using a gentle stream of argon and mounted in a sample holder of the PM-IRRAS setup. PM-IRRAS spectra were recorded using the Bruker Optics PMA50 external module in conjunction with the TENSOR 27 FT-IR spectrometer. A liquid nitrogen cooled MCT detector was used in all experiments. The wavelength setting on the photoelastic modulator, Hinds PEM-90, was fixed at 1600 cm^{-1}. Each sample was scanned for 5 minutes with 3 cm^{-1} resolution and an aperture setting of 6 mm. The incident beam angle used in all experiments was 80º.

III. Results And Discussion

Since it is widely accepted that the initial adsorption of proteins from biological fluids onto implantable biomaterial surfaces significantly influences their biocompatibility[44], it is of great interest to investigate the influence of 316LVM surface charge (potential) on the BSA adsorption kinetics. However, it should be noted that the results and discussion presented here are not limited only to biomedical applications, but also to a range of other applications where interaction of proteins with solid surfaces plays an important role (filtration membranes, biochemical reactors, etc.)[45].

Fig. 1 shows a set of selected PM-IRRAS spectra of the 316LVM stainless steel surface for different immersion times in the electrolyte solution containing 1 g L^{-1} of BSA. The spectra were recorded at surface polarization potential of -1.2 V. Similar spectra (trends) were obtained at other investigated potentials (not shown). The two observed bands, amide I and amide II (Fig. 1), are characteristics of all proteins[43]. In this research, the analysis was focused on the amide I band of the PM-IRRAS spectra due to its strong, well defined signal as well as capability of obtaining useful information on kinetics of surface-adsorbed BSA molecules on stainless steel samples.

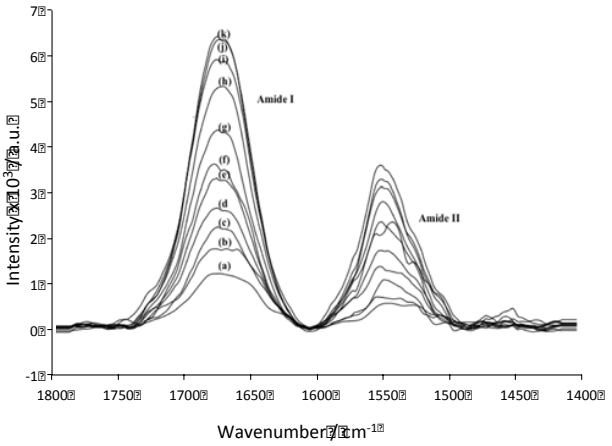

Fig. 1 PM-IRRAS spectra of the 316LVM stainless steel surface following immersion in a phosphate buffer containing 1 g L^{-1} of BSA for increasing cumulative adsorption times: (a) 0.5, (b) 1, (c) 2, (d) 3, (e) 5, (f) 7, (g) 10, (h) 15, (i) 30, (j) 45, and (k) 60 minutes. Electrode (surface) potential = - 1.2 V

It can be seen from the spectra in Fig. 1 that lengthening the immersion time of the stainless steel samples in the BSA solution led to a gradual increase in the overall intensity of the amide I band. Since the area under the amide I peak (integrated intensity) is proportional to the BSA surface concentration, the increase in the peak area in Fig. 1 indicates an increase in surface concentration of the adsorbed protein. This is more clearly observed in eFig. 2, which represents the dependence of integrated intensity of the amide I band on the adsorption time.

The trend observed in Fig. 2 shows that with an increase in adsorption time, the integrated intensity of amide I band also increases, and finally starts leveling off into a quazi-plateau after ca. 20-30 minutes of adsorption. A similar result was obtained in our laboratory for adsorption of fibrinogen onto the same 316LVM surface, at open circuit potential[43], the potential at which no current flows through the cell. McClellan *et al*.[46] have reported that the adsorption density (surface concentration) of BSA on a silicon oxide surface reaches an equilibrium value within 10 minutes for the lowest BSA concentration (0.01 wt%, or ca. 0.1 g L^{-1}), but does not appear to reach an equilibrium value even after 3 hours for the higher concentrations (1 wt%, or ca. 10 g L^{-1}). Sukhishvili *et al.* [47] determined that human serum albumin (HSA) reaches a constant surface concentration on poly-4-vinylpyridine after ca. 30 minutes of adsorption. Similar results were reported in[48] for adsorption of BSA onto a hydrophobic C16 (hexadecyltrichlorosilane) self-assembled monolayer formed on microscope slides. On the other hand, Zeng *et al.*[49] showed that BSA adsorbed on Ti and Ge reaches a quazi-equilibrium surface concentration only after ca. 10 minutes of adsorption, while on a CaP surface the quazi-equilibrium surface concentration was reached after 12 minutes of adsorption from a 20 g L^{-1} BSA solution in saline. Thus, the presented in Fig. 2 agrees well with the corresponding literature results.

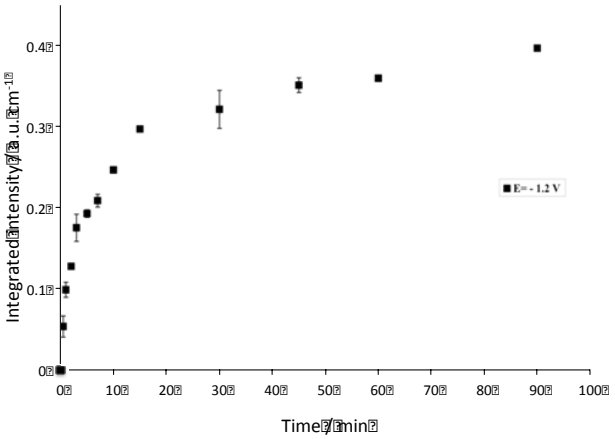

Fig. 2 Dependence of the integrated intensity of amide I band of PM-IRRAS spectra of the 316LVM stainless steel surface on the immersion time in a phosphate buffer containing 1 g L^{-1} of BSA. Applied electrode surface potential = -1.2 V. Symbols (■) represent mean experimental values obtained from PM-IRRAS spectra, while error bars represent the corresponding standard deviation

It would be now interesting to see the effect of surface charge (potential) on the BSA adsorption kinetics and quazi-equilibrium surface concentration. Hence, PM-IRRAS kinetic experiments were performed at different 316LVM WE_2 potentials (from + 0.7 V to - 1.2 V), and the resulting integrated amide I intensity vs. time curves are presented in Fig. 3.

It can be seen from the experimental data presented in the fig. that the integrated intensity of amide I band progressively increases with an increase in immersion time at all investigated potentials, and then levels off into a plateau after

approximately 10-15 minutes, except at -1.2 V (ca. 20-30 min). Another interesting feature to note from the results presented in Fig. 3 is that the adsorbed amount of protein, and hence its surface concentration, increases with an increase in surface potential in the negative direction (cathodic polarization). Therefore, the results in Fig. 3 demonstrate that the 316LVM surface charge (*i.e.* potential) significantly influences the BSA adsorption kinetics and the final (equilibrium / saturated) amount of BSA adsorbed on the surface. This is more clearly presented in Fig. 4, which shows the dependence of the integrated amide I intensity obtained from the plateaus in Fig. 3 on the applied 316LVM surface potential. The graph demonstrates that the dependence between the saturated (equilibrium) surface concentration (integrated amide I intensity) and surface potential is almost linear under the experimental conditions investigated.

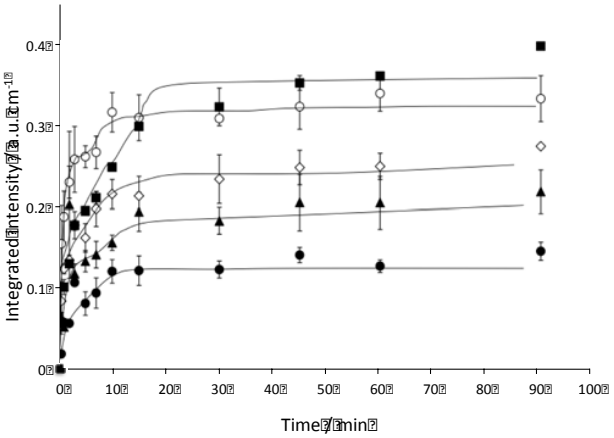

Fig. 3 Dependence of the integrated area of amide I band of PM-IRRAS spectra of the 316LVM stainless steel surface on the immersion time in a phosphate buffer containing 1 g L^{-1} of BSA. The measurements were performed at various WE_2 potentials: (●) + 0.7, (▲) - 0.1, (◊) - 0.5, (○) - 1.0, and (■) - 1.2 V. The solid lines are included only as a visual aid, and do not represent efforts to model the experimental data. Error bars represent the corresponding standard deviation

In spite of BSA being negatively charged at the investigated pH=7.4 (iso-electric point, IEP = 4.7 - 4.9)[50, 51], the favourable adsorption of BSA to a progressively more negative surface, as demonstrated by the results in Fig. 4, suggests that electrostatic interactions do not play a major role in adsorption of BSA onto a hydrophilic 316LVM surface[51]. Favourable adsorption of BSA on negatively charged surfaces was also observed in other studies at different surfaces, such as hydrophilic tin dioxide (SnO_2)[52], carbon[50], and gold[53] surfaces, an no agreement in the literature with respect to the origin of this behaviour is made.

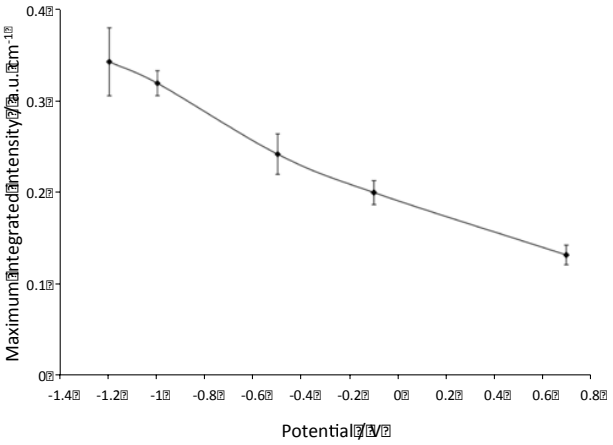

Fig. 4 Dependence of the maximum integrated intensity of amide I band (equilibrium surface concentration) of BSA adsorbed on 316LVM stainless steel samples, on the applied potential. The data was determined from the results in Fig. 3. The data represent the mean value of the last five data points from the plateau of each curve in Fig. 3, while the bars represent the corresponding standard deviation

Martins *et al.*[24] showed that adsorption of HSA on COOH-terminated SAMs, in spite of their hydrophilicity and negative charge at pH 7.4, is higher than on neutral and hydrophilic OH-terminated SAM. Silin *et al.*[54] observed the same behaviour for BSA adsorption on similar monolayers. However, Tidwell *et al.*[55] showed higher albumin adsorption on COOH-terminated SAMs followed in a decreasing order by hydrophobic neutral CH_3- and hydrophilic neutral OH-terminated SAMs. They postulated that although BSA has a net negative charge at neutral pH, its adsorption to negative charged surfaces occurs through positively charged domains on the BSA. Albumin could also bind to negative charged surfaces *via* cationic counter ions acting as an electrostatic bridge[56]. In contrast, some other studies reported a significant influence of surface charge, *i.e.* electrostatic interactions, on protein adsorption[3, 53, 57]. For example, Rezwan *et al.*[58] concluded that electrostatic interaction govern adsorption of BSA and lysozyme for the cases where the protein and the materials surface are very hydrophilic (*e.g.* alumina, silica, and titania). However, for slightly less hydrophilic material surfaces, hydrophobic interaction seems to play an important role in the adsorption process and can even overcome electrostatic repulsion as found for protein adsorption on zirconia.

The authors of this paper currently do not have a firm explanation for the origin of the behaviour seen in Fig. 4, *i.e.* why the adsorption of a negatively-charged BSA molecule is promoted on more negative 316LVM surfaces, but the following explanation could be considered. Previous measurements in the Omanovic laboratory have shown that the electrochemically-treated 316LVM surface used in this project is hydrophilic (contact angle = 35 $\pm 5^{o}$[59], but still the data in Fig. 4 shows that with an increase in surface negative

charge, the surface amount of adsorbed (and negatively charged) BSA molecules also increases. Thus, the *direct* influence of surface wettability is not the driving force for BSA adsorption and its subsequent surface conformation (orientation). However, Omanovic and Roscoe have shown that adsorption of proteins on most surfaces is an entropy-gain driven process[37, 39, 41, 60, 61]. This entropy gain is the result of the dehydration of the protein and surface. Thus, since the BSA molecule sees the 316LVM stainless still surface as less hydrophilic than the surrounding PB aqueous environment, the protein will thus seek to reduce the free energy of the system through adsorption on this surface[62]. Consequently, BSA adsorption will displace highly-ordered dipole water molecules that are aligned at the charged stainless steel surface, thus increasing the disorder of the system at the molecular level and leading to a consequent entropy gain[63]. With an increase in surface potential to more negative values (Fig. 4), the average dipole direction of the water molecular layer on the 316LVM surface becomes more ordered (aligned) with respect to the surface normal, which results in a decrease in the system's entropy (this refers to the situation before BSA adsorbs on the surface). When the BSA molecule adsorbs on the surface, it replaces this well-ordered water molecular layer, which results in an entropy increase, as already mentioned. The more the negative surface is, the larger the difference in entropy of the system at the two states (before and after adsorption), thus larger the adsorption driving force. Recently, Liu *et al.*[64] investigated the adsorption behaviour of various amino acids using hydrophobic interaction chromatography (HIC) and were able to correlate the estimated number of repelled water molecules to the ensuing entropy gain.

In the previous paragraph, and attempt was made to explain why adsorption of a negatively charged BSA molecule is promoted at more negative potentials, but the question is now what the origin of the increased surface concentration of BSA at more negative potentials is (Fig. 4)? A possible explanation could be related to the surface orientation of the BSA molecule. Namely, at positive potentials the molecule is laying on the 316LVM surface in a side-on orientation, which results in the lowest saturated surface concentration of the protein[21]. However, by increasing the negative surface charge of 316LVM (Fig. 4), the BSA molecule gradually rearranges on the surface to adopt an end-on orientation at high negative surface potentials, thus enabling a higher surface concentration to be achieved. This assumption is supported by the fact that the ratio of the BSA surface concentration (*i.e.* the integrated amide I band intensity) in Fig. 4, at -1.2 and 0.7 V is 2.7, which corresponds to the theoretical ratio of saturated BSA surface concentration (mg m^{-2}) in the end-on and side-on orientations, 6.7:2.5 = 2.7[21].

The preceding section discussed the influence of surface potential on the saturated BSA concentration. This is important in situations where equilibrium conditions govern the behaviour of the BSA/316LVM system. However, the initial (short-term) interaction of BSA with the 316LVM surface is also of importance, especially when studying the influence of surface potential on BSA adsorption kinetics. Therefore, the initial BSA adsorption rate $(dA/dt)_{init}$ was determined from the slope of curves in Fig. 3 at short times, and presented in Fig. 5 as a function of surface potential.

The trend at potentials positive of -1.0 V (Fig. 5) is similar to that one presented in Fig. 4. With an increase in the 316LVM surface potential towards negative values, the initial BSA adsorption rate also increased. However, at -1.2 V the initial BSA adsorption rate decreased. The explanation of the trend in the fig. can be based on the explanation of the trend in Fig. 4, previously discussed. Namely, with the increase in surface potential towards negative values, the entropy of water molecules at the electrode surface decreases due to the increase in their surface order, while the electrostatic bond between the negatively charged surface and positively charged hydrogen atoms increases. However, when BSA adsorbs on the 316LVM surface, it displaces the water molecules arranged on the charged substrate surface, but also the water molecules that solvate the hydrophilic BSA pockets, which then gets in contact with the 316LVM surface. These highly ordered water molecules go into the solution, the process that results in a significant increase in entropy of the system. The more negative surface potential is, the higher the order of the system is, and thus the higher the entropy gain resulting from BSA adsorption is, leading to the higher adsorption driving force. The decrease in initial BSA adsorption rate at -1.2V might be due to the parallel occurrence of hydrogen evolution reaction on the 316LVM surface[59]. The first step in this reaction is the adsorption of hydrogen on the surface to make a metal-hydrogen bond ($M\text{-}H_{ads}$)[65-67]. The hydrogen-covered ('blocked') 316LVM surface (-1.2 V) offers different physico-chemical properties (wettability, charge and chemistry) than the naked and solvated 316LVM surface (≥ -1.0 V), which in turns influences (decreases) the initial BSA adsorption rate.

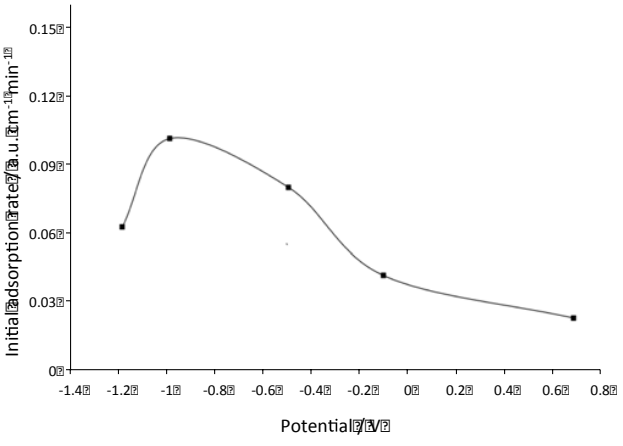

Fig. 5 Dependence of the initial BSA adsorption rate on 316LVM stainless steel on the applied surface potential. The data was obtained from the results in Fig. 3

IV. Conclusions

It was demonstrate that PM-IRRAS can be efficiently used to investigate protein/surface adsorptive interactions. The kinetics of BSA adsorption on the 316LVM surface greatly depends on the surface potential. With an increase in surface potential towards more negative values, the initial adsorption rate also increases, reaching a maximum at -1.0 V. The trend was explained on the basis of replacement of well-ordered water molecules at the 316LVM/solution interface, *i.e*. by the increase in adsorption driving force (entropy gain) with negative potentials. At more negative potentials, adsorption of BSA competes with the hydrogen evolution reaction, resulting in a slight decrease in initial BSA adsorption rate. At each potential, BSA reaches a saturated surface coverage (concentration) after approximately 10-30 minutes of adsorption, depending on the potential. This time thus corresponds to the time needed for the system to reach equilibrium. Similarly to the initial adsorption rate, the saturated surface concentration of BSA also increases with negative surface potential. This trend was explained on the basis of the change in orientation of the BSA molecule on the surface, from the side-on orientation at more positive potentials, to the end-on orientation at more negative potentials.

This research is expected to make contribution to the fundamental knowledge on protein/surface interactions. It has shed some light on the influence of surface charge (potential) on BSA adsorption. This can contribute to development of new biomedical and industrial materials, devices and processes.

References

[1] Pasche S, Voros J, Griesser HJ, Spencer ND, Textor M. Effects of ionic strength and surface charge on protein adsorption at PEGylated surfaces. Journal of Physical Chemistry B 2005;109: 17545-52.

[2] Martins MCL, Wang D, Ji J, Feng L, Barbosa MA. Albumin and fibrinogen adsorption on PU-PHEMA surfaces. Biomaterials 2003;24: 2067-76.

[3] Moulton SE, Barisci JN, Bath A, Stella R, Wallace GG. Investigation of protein adsorption and electrochemical behavior at a gold electrode. Journal of Colloid and Interface Science 2003;261: 312-9.

[4] Trojanowicz M, Krawczyk TKV. Electrochemical Biosensors Based on Enzymes Immobilized in Electropolymerized Films. Mikrochimica Acta 1995;121: 167-81.

[5] Cornelius RM, Wojciechowski PW, Brash JL. Measurement of Protein Adsorption-Kinetics by An Insitu, Real-Time, Solution Depletion Technique. Journal of Colloid and Interface Science 1992;150: 121-33.

[6] Fukuzaki S, Urano H, Nagata K. Adsorption of Protein Onto Stainless-Steel Surfaces. Journal of Fermentation and Bioengineering 1995;80: 6-11.

[7] Noh H, Vogler EA. Volumetric interpretation of protein adsorption: Competition from mixtures and the Vroman effect. Biomaterials 2007;28: 405-22.

[8] Weber N, Wendel HP, Ziemer G. Hemocompatibility of heparin-coated surfaces and the role of selective plasma protein adsorption. Biomaterials 2002;23: 429-39.

[9] Burns NL, Holmberg K, Brink C. Influence of Surface Charge on Protein Adsorption at An Amphoteric Surface - Effects of Varying Acid to Base Ratio. Journal of Colloid and Interface Science 1996;178: 116-22.

[10] Bentaleb A, Abele A, Haikel Y, Schaaf P, Voegel JC. FTIR-ATR and radiolabeling study of structural modifications during protein adsorption on hydrophilic surfaces. 2. The Case of apo-alpha-lactalbumine. Langmuir 1999;15: 4930-3.

[11] Price ME, Cornelius RM, Brash JL. Protein adsorption to polyethylene glycol modified liposomes from fibrinogen solution and from plasma. Biochimica et Biophysica Acta - Biomembranes 2001;1512: 191-205.

[12] Seitz R, Brings R, Geiger R. Protein adsorption on solid-liquid interfaces monitored by laser-ellipsometry. Applied Surface Science 2005;252: 154-7.

[13] Hook F, Voros J, Rodahl M, Kurrat R, Boni P, Ramsden JJ et al. A comparative study of protein adsorption on titanium oxide surfaces using in situ ellipsometry, optical waveguide lightmode spectroscopy, and quartz crystal microbalance/dissipation. Colloids and Surfaces B-Biointerfaces 2002;24: 155-70.

[14] Armstrong J, Salacinski HJ, Mu QS, Seifalian AM, Peel L, Freeman N et al. Interfacial adsorption of fibrinogen and its inhibition by RGD peptide: a combined physical study. Journal of Physics-Condensed Matter 2004;16: S2483-S91.

[15] Toscano A, Santore MM. Fibrinogen adsorption on three silica-based surfaces: Conformation and kinetics. Langmuir 2006;22: 2588-97.

[16] Ngankam AP, Mao GZ, Van Tassel PR. Fibronectin adsorption onto polyelectrolyte multilayer films. Langmuir 2004;20: 3362-70.

[17] Wegner GJ, Wark AW, Lee HJ, Codner E, Saeki T, Fang SP et al. Real-time surface plasmon resonance imaging measurements for the multiplexed determination of protein adsorption/desorption kinetics and surface enzymatic reactions on peptide microarrays. Analytical Chemistry 2004;76: 5677-84.

[18] Evans-Nguyen KM, Fuierer RR, Fitchett BD, Tolles LR, Conboy JC, Schoenfish MH. Changes in adsorbed fibrinogen upon conversion to fibrin Langmuir 2006;22: 5115-21.

[19] Forciniti D, Hamilton WA. Surface enrichment of proteins at quartz/water interfaces: A neutron reflectivity study. Journal of Colloid and Interface Science 2005;285: 458-68.

[20] Petrash S, Cregger T, Zhao B, Pokidysheva E, Foster MD, Brittain WJ et al. Changes in protein adsorption on self-assembled monolayers with monolayer order: Comparison of human serum albumin and human gamma globulin. Langmuir 2001;17: 7645-51.

[21] Cosman NP, Roscoe SG. Electrochemical quartz crystal nanobalance (EQCN) studies of protein interfacial behavior at Pt. Langmuir 2004;20: 1711-20.

[22] Wright JEI, Cosman NP, Fatih K, Omanovic S, Roscoe SG. Electrochemical impedance spectroscopy and quartz crystal nanobalance (EQCN) studies of insulin adsorption on Pt. Journal of Electroanalytical Chemistry 2004;564: 185-97.

[23] Hemmersam AG, Foss M, Chevallier J, Besenbacher F. Adsorption of fibrinogen on tantalum oxide, titanium oxide and gold studied by the QCM-D technique. Colloids and Surfaces B-Biointerfaces 2005;43: 208-15.

[24] Martins MCL, Fonseca C, Barbosa MA, Ratner BD. Albumin adsorption on alkanethiols self-assembled monolayers on gold electrodes studied by chronopotentiometry. Biomaterials 2003;24: 3697-706.

[25] Ithurbide A, Frateur I, Galtayries A, Marcus P. XPS and flow-cell EQCM study of albumin adsorption on passivated chromium surfaces: Influence of potential and pH. Electrochimica Acta 2007;53: 1336-45.

[26] Wagner MS, Castner DG. Analysis of adsorbed proteins by static time-of-flight secondary ion mass spectrometry. Applied Surface Science 2004;231-2: 366-76.

[27] Ademovic Z, Klee D, Kingshott P, Kaufmann R, Hocker H. Minimization of protein adsorption on poly(vinylidene fluoride). Biomolecular Engineering 2002;19: 177-82.

[28] Li LY, Chen SF, Jiang SY. Protein adsorption on alkanethiolate self-assembled monolayers: Nanoscale surface structural and chemical effects. Langmuir 2003;19: 2974-82.

[29] Tunc S, Maitz MF, Steiner G, Vazquez L, Pham MT, Salzer R. In situ conformational analysis of fibrinogen adsorbed on Si surfaces. Colloids and Surfaces B-Biointerfaces 2005;42: 219-25.

[30] Rodrigues SN, Goncalves IC, Martins MCL, Barbosa MA, Ratner BD. Fibrinogen adsorption, platelet adhesion and activation on mixed hydroxyl-/methyl-terminated self-assembled monolayers. Biomaterials 2006;27: 5357-67.

[31] Song L, Meng J, Zhong J, Liu LF, Dou XY, Liu DF et al. Human fibrinogen adsorption onto single-walled carbon nanotube films. Colloids and Surfaces B-Biointerfaces 2006;49: 66-70.

[32] Schwinte P, Voegel JC, Picart C, Haikel Y, Schaaf P, Szalontai B. Stabilizing effects of various polyelectrolyte multilayer films on the

structure of adsorbed/embeded fibrinogen molecules: An ATR-FTIR study. Journal of Physical Chemistry B 2001;105: 11906-16.
[33] Roach P, Farrar D, Perry CC. Interpretation of protein adsorption: Surface-induced conformational changes. Journal of the American Chemical Society 2005;127: 8168-73.
[34] Frateur I, Lartundo-Rojas L, Methivier C, Galtayries A, Marcus P. Influence of bovine serum albumin in sulphuric acid aqueous solution on the corrosion and the passivation of an iron-chromium alloy. Electrochimica Acta 2006;51: 1550-7.
[35] Desroches MJ, Chaudhary N, Omanovic S. PM-IRRAS investigation of the interaction of serum albumin and fibrinogen with a biomedical-grade stainless steel 316LVM surface. Biomacromolecules 2007;8: 2836-44.
[36] Omanovic S, Roscoe SG. Electrochemical studies of the adsorption behavior of bovine serum albumin on stainless steel. Langmuir 1999;15: 8315-21.
[37] Jackson DR, Omanovic S, Roscoe SG. Electrochemical studies of the adsorption behavior of serum proteins on titanium. Langmuir 2000;16: 5449-57.
[38] Cabilio NR, Omanovic S, Roscoe SG. Electrochemical studies of the effect of temperature and pH on the adsorption of alpha-lactalbumin at Pt. Langmuir 2000;16: 8480-8.
[39] Cosman NP, Fatih K, Roscoe SG. Electrochemical impedance spectroscopy study of the adsorption behaviour of alpha-lactalbumin and beta-casein at stainless steel. Journal of Electroanalytical Chemistry 2005;574: 261-71.
[40] Omanovic S, Roscoe SG. Interactive adsorption behavior of beta-lactoglobulin and linoleate at a 316L stainless steel surface. Electrochemical and Solid State Letters 2005;8: E12-E5.
[41] Omanovic S, Roscoe SG. Interfacial behavior of beta-lactoglobulin at a stainless steel surface: An electrochemical impedance spectroscopy study. Journal of Colloid and Interface Science 2000;227: 452-60.
[42] Kwok KC, Yeung KM, Cheung NH. Adsorption kinetics of bovine serum albumin on fused silica: Population heterogeneities revealed by single-molecule fluorescence microscopy. Langmuir 2007;23: 1948-52.
[43] Desroches MJ, Omanovic S. Adsorption of fibrinogen on a biomedical-grade stainless steel 316LVM surface: a PM-IRRAS study of the adsorption thermodynamics, kinetics and secondary structure changes. Physical Chemistry Chemical Physics 2008;10: 2502-12.
[44] Wahlgren M, Arnebrant T. Protein Adsorption to Solid-Surfaces. Trends in Biotechnology 1991;9: 201-8.
[45] Maruyama T, Katoh S, Nakajima M, Nabetani H, Abbott TP, Shono A, et al. FT-IR analysis of BSA fouled on ultrafiltration and microfiltration membranes. Journal of Membrane Science 2001;192: 201-7.
[46] McClellan SJ, Franses EI. Adsorption of bovine serum albumin at solid/aqueous interfaces. Colloids and Surfaces A-Physicochemical and Engineering Aspects 2005;260: 265-75.
[47] Sukhishvili SA, Granick S. Adsorption of human serum albumin: Dependence on molecular architecture of the oppositely charged surface. Journal of Chemical Physics 1999;110: 10153-61.
[48] Wertz CF, Santore MM. Adsorption and relaxation kinetics of albumin and fibrinogen on hydrophobic surfaces: Single-species and competitive behavior. Langmuir 1999;15: 8884-94.
[49] Zeng HT, Chittur KK, Lacefield WR. Analysis of bovine serum albumin adsorption on calcium phosphate and titanium surfaces. Biomaterials 1999;20: 377-84.
[50] Bernabeu P, Caprani A. Influence of surface charge on adsorption of fibrinogen and/or albumin on a rotating disc electrode of platinum and carbon. Biomaterials 1990;11: 258-64.
[51] Bos MA, Shervani Z, Anusiem ACI, Giesbers M, Norde W, Kleijn JM. Influence of the electric potential of the interface on the adsorption of proteins. Colloids Surfaces B: Biointerfaces 1994;3: 91-100.
[52] Asanov AN, Delucas LJ, Oldham PB, Wilson WW. Heteroenergetics of Bovine Serum Albumin Adsorption from Good Solvents Related to Crystallization Conditions. Journal of Colloid and Interface Science 1997;191: 222-35.
[53] Brewer SH, Glomm WR, Johnson MC, Knag MK, Franzen S. Probing BSA binding to citrate-coated gold nanoparticles and surfaces. Langmuir 2005;21: 9303-7.
[54] Silin V, Weetall H, Vanderah DJ. SPR studies of the nonspecific adsorption kinetics of human IgG and BSA on gold surfaces modified by self-assembled monolayers (SAMs). Journal of Colloid and Interface Science 1997;185: 94-103.
[55] Tidwell CD, Ertel SI, Ratner BD, Tarasevich BJ, Atre S, Allara DL. Endothelial Cell Growth and Protein Adsorption on Terminally Functionalized, Self-Assembled Monolayers of Alkanethiolates on Gold. Langmuir 1997;13: 3404-13.
[56] Dent AH, Aslam M. Other categories of protein coupling. Bioconjugation: Protein Coupling Techniques for the Biomedical Sciences. Edited by Aslam M, Dent AH. London: Macmillan Reference; 1998: 504–69.
[57] Yin G, Liu Z, Zhan J, Ding FX, Yuan NJ. Impacts of the surface charge property on protein adsorption on hydroxyapatite. Chemical Engineering Journal 2002;87: 181-6.
[58] Rezwan K, Studart AR, Voros J, Gauckler LJ. Change of ζ potential of biocompatible colloidal oxide particles upon adsorption of bovine serum albumin and lysozyme. Journal of Physical Chemistry B 2005;109: 14469-74.
[59] Shahryari A. Nhancement of Biocompatibility of 316LVM Stainless Steel by Electrochemical Cyclic Potentiodynamic Passivation. Ph.D. Thesis. McGill University; 2008.
[60] Pyshnov E, Farcas M, Cosman N, Roscoe SG, Omanovic S. The Cell Biomaterial Reaction. European Cells and Materials Journal 2004;7(suppl. 1): 80.
[61] Desroches MJ. Electrochemical and PM-IRRAS studies of the interaction of plasma protein fibrinogen with a biomedical-grade 316LVM stainless steel surface. Master. Thesis. McGill University; 2007.
[62] Nadarajah A, Lu CF, Chittur KK. Modeling the Dynamics of Protein Adsorption to Surfaces. Proteins at Interfaces II: Fundamentals and Applicactions. Edited by Horbett TA, Brash JL. Washington, D.C: American Chemical society; 1995: 181-94.
[63] Norde W. Adsorption of Proteins from Solution at the Solid-Liquid Interface. Advances in Colloid and Interface Science 1986;25: 267-340.
[64] Liu CI, Hsu KY, Ruaan RC. Hydrophobic contribution of amino acids in peptides measured by hydrophobic interaction chromatography. Journal of Physical Chemistry B 2006;110: 9148-54.
[65] Damian A, Omanovic S. Ni and Ni-Mo hydrogen evolution electrocatalysts electrodeposited in a polyaniline matrix. Journal of Power Sources 2006;158: 464-76.
[66] Navarro-Flores E, Chong ZW, Omanovic S. Characterization of Ni, NiMo, NiW and NiFe electroactive coatings as electrocatalysts for hydrogen evolution in an acidic medium. Journal of Molecular Catalysis A-Chemical 2005;226: 179-97.
[67] Navarro-Flores E, Omanovic S. Hydrogen evolution on nickel incorporated in three-dimensional conducting polymer layers. Journal of Molecular Catalysis A-Chemical 2005;242: 182-94.